

Model-predictive control based on Harris Hawks optimization for split-source inverter

Youssef Elthokaby¹, Ibrahim Abdelsalam², Naser Abdel-Rahim³, Islam Mohamed Abdelqawee¹

¹Department of Electrical Engineering, Faculty of Engineering at Shoubra, Benha University, Cairo, Egypt

²Department of Electrical Engineering, College of Engineering and Technology, Arab Academy for Science and Technology and Maritime Transport, Cairo, Egypt

³Department of Electrical Engineering, Faculty of Engineering & Technology, Future University, New Cairo, Egypt

Article Info

Article history:

Received Mar 17, 2022

Revised May 15, 2022

Accepted June 26, 2022

Keywords:

Cost function

Discrete time model

Model predictive control

Optimization technique

Split-source inverter

ABSTRACT

This paper proposed a modified algorithm for controlling a single-phase split-source inverter. The proposed algorithm is a modified model predictive control based on Harris Hawks optimization, where the AC output voltage, the DC-link voltage, and the DC input current are controlled within one cost function. Hence, the discrete time models of both AC-side and DC-side are obtained. For proper operation of the modified MPC, each error term within the cost function has a weighting factor. Harris Hawks optimization technique is used to determine the weighting factors at each term of the cost function. The proposed algorithm is validated using MATLAB/Simulink. Simulation results show that the system has succeeded in controlling AC load voltage, input current, and achieving constant DC-link voltage over a wide operating range.

This is an open access article under the [CC BY-SA](https://creativecommons.org/licenses/by-sa/4.0/) license.



Corresponding Author:

Youssef Elthokaby

Department of Electrical Engineering, Faculty of Engineering at Shoubra, Benha University

Cairo, Egypt

Email: youssef.hassan@feng.bu.edu.eg

1. INTRODUCTION

The interest in single-stage topologies in the last years has been grown due to the need to reduce size, cost and increase the efficiency of the power converters [1], [2]. The single-stage topology must perform two functions: 1) controlling the dc voltage and 2) ensuring that the output AC voltage is sinusoidal with low THD. Z-source inverter (ZSI) is a single-stage converter with buck-boost characteristic property. All switching states of the VSI is used in the ZSI in addition to a shoot-through state. ZSI suffers from many drawbacks such as, unidirectional power flow, high inrush current during starting, and discontinuous input current [3]. The researchers try to solve these drawbacks in two ways. The first way, by changing the configuration of the impedance network [3]-[6]. The second was, by improving a proper control strategy for various application requirements [7]. The number of passive components in the impedance network of ZSI such as inductors and capacitors are relatively large.

Split source inverter (SSI) is a single-stage boosting converter which has different circuit topologies in literature [8]-[12]. SSI has the capability of using the same switching states as the VSI for its basic operation and there is no need for extra states [8]. SSI provide advantages over the existing single-stage topologies as: 1) continuous dc-link voltage, 2) continuous input dc current, 3) lower passive components count, 4) using the same standard modulation schemes as the VSI for its basic operation. On the other hand, it suffers from the following disadvantages: 1) a sufficient dead band time should be generated, 2) unequal current distribution among the different switches [9].

In literature, SSI uses traditional PWM with PI controller which suffers from the low response and minimum phase [9]-[12]. Model predictive control (MPC) is presented with the high-performance response and no minimum phase problem [13]-[15]. MPC is a controller, which uses the discrete-time model of the system to predict the future behavior of the controlled variables for all possible voltage vectors of the converter. The predicted variables are then used to obtain optimal action by choosing the voltage vector that minimizes a predefined cost function [16]. Hence, it is more suitable for the discrete nature of the power electronics converters, and it lends itself easier to its application [17]-[20]. MPC has many advantages such as: 1) it is easy to understand, 2) it can be applied to a wide variety of systems, 3) it deals with multivariable cases, and nonlinearities [21], and 4) capable of using constraints [22]-[24].

In this paper, finite control-set model predictive control (FCS-MPC) is modified to control the AC and DC sides of the single-phase SSI. The cost function consists of output AC voltage error, DC-link voltage error, and DC input current error. Hence, only one cost function has been used to control the three variables. For proper operation of the modified MPC, weighting factors are used within the cost function. Harris Hawks optimization (HHO) technique is used to determine the optimal values of the weighting factors.

2. FINITE CONTROL-SET MODEL PREDICTIVE CONTROL FOR SPLIT-SOURCE INVERTER

The single-phase SSI employed in this paper is shown in Figure 1 [10]. The principle of operation is described with the aid of Figure 2 and Figure 3 as follows. When the switch Q_5 is turned ON the inductor L_{dc} is charged (see Figure 2), and the SSI can operate with all possible output voltage ($+V_{inv}$, $-V_{inv}$, and zero). The inductor L_{dc} is discharging into the capacitor (C_{dc}) when the switch Q_5 is turned OFF. At this moment, the SSI can operate with only two possible outputs ($+V_{inv}$ and zero) as shown in Figure 3. The DC-link voltage (V_{inv}) is function of the duty cycle of switch Q_5 and is given by (1).

$$v_{inv} = \frac{v_{dc}}{1-D} \quad (1)$$

In order to design FCS-MPC, the following steps are required: 1) the system model, 2) the discrete time model, and 3) the cost function.

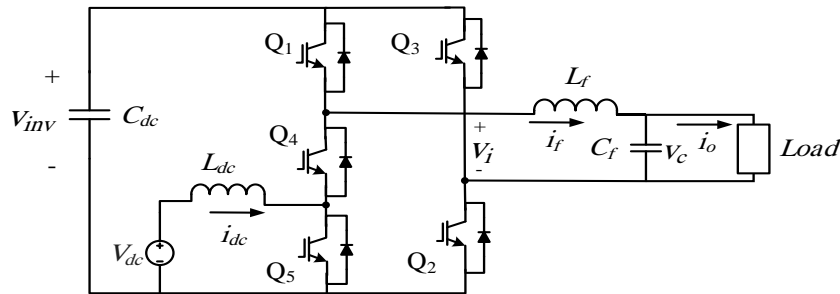


Figure 1. Single-phase SSI system

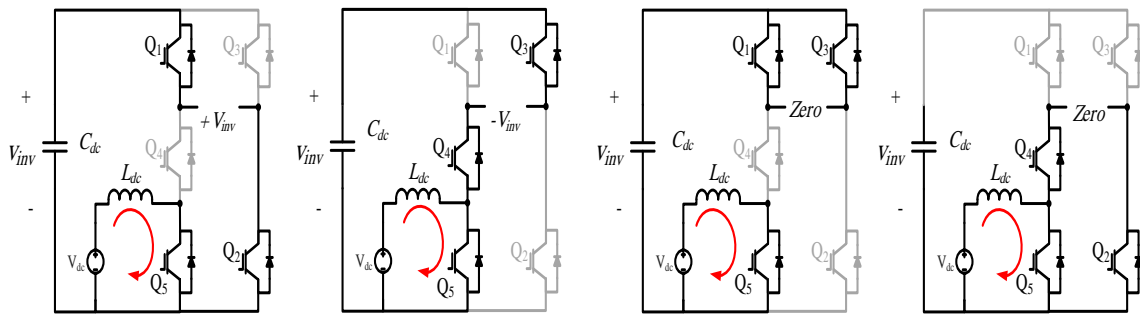


Figure 2. Possible switching states of the single-phase SSI at charging L_{dc}

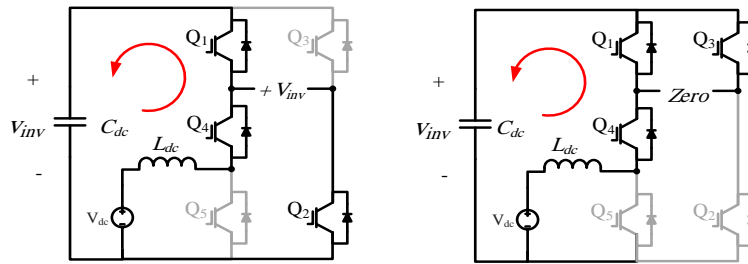


Figure 3. Possible switching states of the single-phase SSI at discharging L_{dc}

2.1. System model and discrete time model

2.1.1. AC side model

The governing differential equations of the LC filter variables are:

$$L_f \frac{di_f}{dt} = v_i - v_c \quad (2)$$

$$C_f \frac{dv_c}{dt} = i_f - i_o \quad (3)$$

where, v_c is the AC load voltage, v_i is the inverter output voltage which applied to the filter, i_f is the filter inductor current, i_o is the AC load current, C_f is the filter capacitance, and L_f is the filter inductance.

The equations can be rewritten in a state-space system form as:

$$\frac{dx}{dt} = Ax + Bv_i + B_d i_o \quad (4)$$

where,

$$x = [i_f \quad v_c]^T \quad (5)$$

$$A = \begin{bmatrix} 0 & -\frac{1}{L_f} \\ \frac{1}{C_f} & 0 \end{bmatrix}, B = \begin{bmatrix} \frac{1}{L_f} \\ 0 \end{bmatrix}, \text{ and } B_d = \begin{bmatrix} 0 \\ -\frac{1}{C_f} \end{bmatrix} \quad (6)$$

The output voltage expressed in a vector-matrix form is given as:

$$v_c = [0 \quad 1]x \quad (7)$$

The discrete time model is obtained from (4) for a sampling time T_s and expressed as:

$$x(k+1) = A_q x(k) + B_q v_i(k) + B_{dq} i_o(k) \quad (8)$$

where,

$$A_q = e^{AT_s}, B_q = \int_0^{T_s} e^{At} B dt, \text{ and } B_{dq} = \int_0^{T_s} e^{At} B_d dt \quad (9)$$

2.1.2. DC side model

The DC side of the single-phase SSI consists of an input inductor (L_{dc}) and DC-link capacitor (C_{dc}). The governing equations of the DC side has two cases depending on the state of switch Q_5 [25]-[27]. Case one, the switch Q_5 is turned on and the input inductor (L_{dc}) is charging as shown in Figure 4(a). The dynamic equation of the input inductor current and the DC-link capacitor voltage can be presented as:

$$V_{dc} = L_{dc} \frac{di_{dc}}{dt} \quad (10)$$

$$i_f = C_{dc} \frac{dV_{inv}}{dt} \quad (11)$$

Where, V_{dc} is the input DC voltage, i_{dc} is the input DC current, and V_{inv} is the DC-link voltage. For first order system, the discrete time model is obtained by simple Euler approximation as:

$$\frac{dx}{dt} = \frac{x(k+1) - x(k)}{T_s} \quad (12)$$

Hence, the discrete time model of the input inductor current and the DC-link capacitor voltage are:

$$i_{dc}(k+1) = i_{dc}(k) + \frac{T_s}{L_{dc}} V_{dc}(k) \quad (13)$$

$$V_{inv}(K+1) = V_{inv}(k) + \frac{T_s}{C_{dc}} i_f \quad (14)$$

Case two, the switch Q_5 is turned off and the input inductor (L_{dc}) is discharging as shown in Figure 4(b). The dynamic equation of the input inductor current and DC-link capacitor voltage can be presented as:

$$V_{dc} - V_{inv} = L_{dc} \frac{di_{dc}}{dt} \quad (15)$$

$$i_{dc} - i_f = C_{dc} \frac{dV_{inv}}{dt} \quad (16)$$

The discrete time model of the input inductor current and the DC-link capacitor voltage are:

$$i_{dc}(k+1) = i_{dc}(k) + \frac{T_s}{L_{dc}} (V_{dc}(k) - V_{inv}(k)) \quad (17)$$

$$V_{inv}(K+1) = V_{inv}(k) + \frac{T_s}{C_{dc}} (i_{dc}(k) - i_f(k)) \quad (18)$$

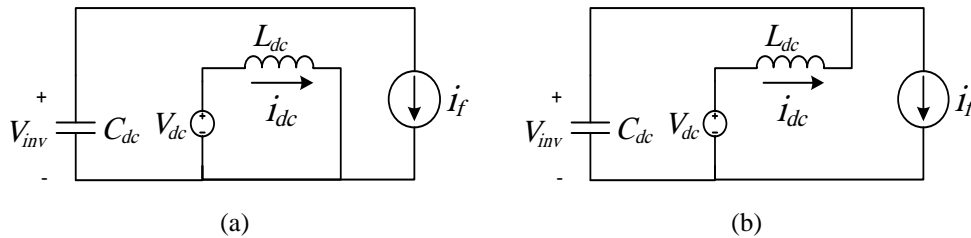


Figure 4. The two cases of the SSI circuits at (a) Q_5 is turned on and (b) Q_5 is turned off

2.2. Model predictive control strategy

In this section, the MPC controller is modified to generate the switching action for the single-phase SSI switches according to input power, DC-link voltage, and AC output voltage. The duty cycle of switch Q_5 is determined inside the MPC controller. The modified MPC algorithm for the single-phase SSI system is shown in Figure 5. At any instance (k) and from knowing the current states of the DC-link voltage (V_{inv}) and DC input current (i_{dc}), these variables can be predicted in both ON state and OFF state of the switch Q_5 . In the ON state, The DC input current (i_{dc}) and the DC-link voltage (V_{inv}) are predicted from (13) and (14). The single-phase SSI can operate with all possible voltage vectors as shown in Figure 2. The cost function g_{on} is used to calculate the error between each of the predicted variables and their reference values. The cost function consists of the AC side error, the DC-link error, and the DC input current error as in (19). Weighting factors are used for the proper operation of the modified MPC. Harris Hawks optimization (HHO) technique is used to calculate the weighting factors. The voltage vector that minimized the cost function (g_{on}) is stored. In the OFF state, the DC input current (i_{dc}) and the DC-link voltage (V_{inv}) are predicted from (17) and (18). The single-phase SSI can operate with two possible voltage vectors as shown in Figure 3. The cost function (g_{off}) is used to obtain the optimal voltage vector at OFF state as in (20). In both ON and OFF states the output AC voltage is predicted from (8). The optimal voltage vector from the ON state is compared with the optimal vector of the OFF state, and the vector that has minimal error is chosen to apply in the next sample.

$$g_{on} = w_1 |v_c^* - v_c(k+1)| + w_2 |V_{inv}^* - V_{inv}(k+1)| + w_3 |i_{dc}^* - i_{dc}(k+1)| \quad (19)$$

$$g_{off} = w_1 |v_c^* - v_c(k+1)| + w_2 |V_{inv}^* - V_{inv}(k+1)| + w_3 |i_{dc}^* - i_{dc}(k+1)| \quad (20)$$

where, w_1 is the weighting factor of the AC load voltage error, w_2 is the weighting factor of the DC-link voltage error, and w_3 is the weighting factor of the DC input current error.

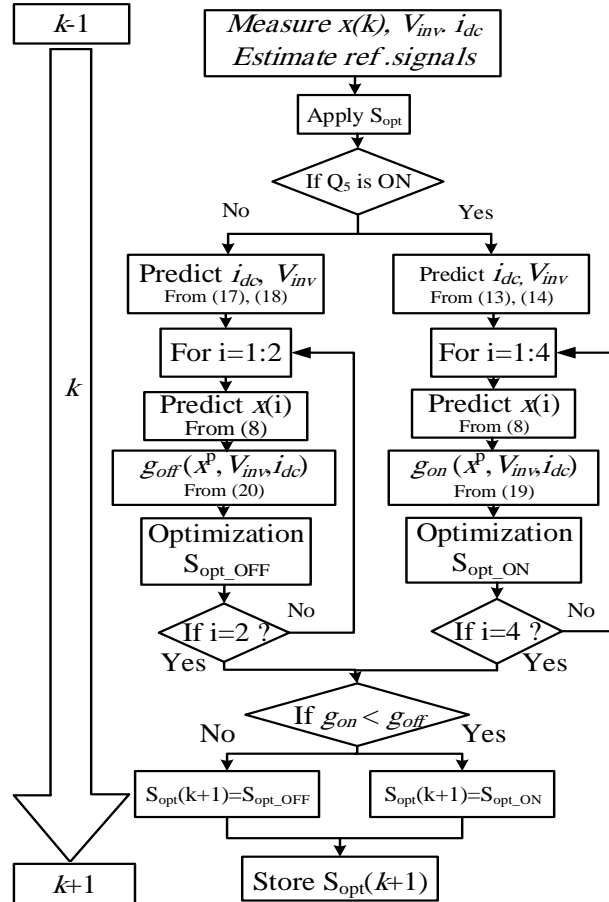


Figure 5. FCS-MPC algorithm

3. HARRIS HAWK OPTIMIZATION

Harris Hawks optimization (HHO) technique is used to obtain the weighting factors of the cost function. The integration of absolute error (IAE) of AC load voltage error, e_{vac} , the DC-link voltage error, e_{vdc} and the error current in the DC input current, e_{idc} , are used as the objective function (21). As shown in Figure 6, HHO mimics the Harris hawks' cooperation behavior in chasing the prey, which is called surprise pounce [28]. The optimized values of the weighting factor are the prey that hawks tend to catch. As any optimization technique, HHO consists of the exploration and exploitation phases. In the exploration phase, the hawks intend to detect and track the prey by searching in some random areas. As the prey energy decreases, the algorithm transits from exploration phase to exploitation phase. In the exploitation phase, the Hawks attack the intended prey detected in the previous phase by performing the surprise pounce [29].

$$IAE = \int_0^\infty |e_{vac}(t)|dt + \int_0^\infty |e_{vdc}(t)|dt + \int_0^\infty |e_{idc}(t)|dt \quad (21)$$

where,

$$e_{vac} = v_c^* - v_c, e_{vdc} = V_{inv}^* - V_{inv}, \text{ and } e_{idc} = i_{dc}^* - i_{dc} \quad (22)$$

<pre> INPUT Number of search agents n, the number of iterations T, dimensional space D Initialize the position of hawks Y_i ($i=1, 2, \dots, n$) WHILE the end condition is not satisfied FOR $i = 1 : n$ Calculate the objective function value of each hawk through (25) Update the position of the intended prey Y_{prey} END FOR FOR $i = 1 : n$ Update the initial energy E_0, jump strength J Update the escaping energy $E = 2E_0(1 - \frac{t}{T})$ IF $E \geq 1$ (Exploration phase) IF $K = rand() < 0.5$ Update the position of the hawk $Y(t+1) = Y_{prey}(t) - Y_m(t) - c_3(LB + c_4(LB - LB))$ ELSE Update the position of the hawk $Y(t+1) = Y_{rand}(t) - c_1 Y_{rand}(t) - 2c_2 Y(t)$ END IF END IF IF $E < 1$ (Exploitation phase) IF $r \geq 0.5$ and $E \geq 0.5$ (Soft besiege) Update the position of the hawk $Y(t+1) = (Y_{prey}(t) - Y(t)) - E Y_{prey}(t) - Y(t)$ ELSE IF $r \geq 0.5$ and $E < 0.5$ (Hard besiege) Update the position of the hawk $Y(t+1) = Y_{prey}(t) - E Y_{prey}(t) - Y(t)$ ELSE IF $r < 0.5$ and $E \geq 0.5$ (Soft besiege with progressive rapid dives) Update the position of the hawk $Y(t+1) = \begin{cases} Y_{prey}(t) - E Y_{prey}(t) - Y(t) & \text{if } F(H) < F(Y(t)) \\ H + S \times LF(D) & \text{if } F(G) < F(Y(t)) \end{cases}$ ELSE IF $r < 0.5$ and $E < 0.5$ (Hard besiege with progressive rapid dives) Update the position of the hawk $Y(t+1) = \begin{cases} Y_{prey}(t) - E Y_{prey}(t) - Y_m(t) & \text{if } F(H) < F(Y(t)) \\ H + S \times LF(D) & \text{if } F(G) < F(Y(t)) \end{cases}$ END IF END IF Check and correct the new positions based on the boundaries of variables END FOR END WHILE RETURN Y_{prey}, which represents the optimal values </pre>	<p>Where</p> <p>E_0 is the initial state of the prey energy</p> <p>t is the current iteration counter</p> <p>T is the max iteration</p> <p>K is a random number inside (0,1), indicates the position of the hawk according to the position of other team members</p> <p>c_1, c_2, c_3, c_4 are random numbers inside (0,1) updated in each iteration</p> <p>$Y(t)$ is the current position vector of hawks</p> <p>$Y_{rand}(t)$ is a randomly selected hawk from the current population</p> <p>$Y_m(t)$ is the average position of the hawks,</p> <p>LB & UB are the lower and upper bounds of variables</p> <p>r is the chance of a prey in successfully escaping</p> <p>D is the dimension of the problem</p> <p>S is a random vector by size $1 \times D$</p> <p>LF is the Lévy flight function</p> <p>J refers to the strength of the prey randomly jumping during the escape</p>
---	---

Figure 6. Pseudo code of Harris Hawks optimization

4. SIMULATION RESULTS

The single-phase SSI, shown in Figure 1, is simulated using MATLAB/Simulink. The system parameters shown in Table 1. The modified MPC is used to control the single-phase SSI where all the five switches (Q1-Q5) are controlled. The AC output reference voltage is chosen to be 220 V, 50 Hz. The DC-link reference voltage and the input reference current are chosen to be 500 V, and 8.5 A (1200 W) respectively. The weighting factors (in (19) and (20)) are obtained by HHO and equal to $w_1=1$, $w_2=0.16$, and $w_3=0.11$. The AC output voltage waveform (v_c) is shown in Figure 7. The output voltages are sinusoidal with low THD of 1.49% and peak value equal to 311 V as shown in Figure 8. Figure 9 shows the load currents (i_o), which equals 5.5 A rms. The load consumed nearly 1200 W from the supply. The DC-link voltage (V_{inv}) is shown in Figure 10, and equal to 495 V with low ripples (less than 2%). The DC input inductor current (i_{dc}) is shown in Figure 11 and has average value equals 8.5 A. The results show that more than one variable can be controlled with MPC with proper selection of weighting factors. And this is the most important feature of the MPC over other controllers.

The dynamic behavior of the single-phase system is investigated by applying sudden change in the load from 40 Ω to 20 Ω (100% load change) at 11.05 sec as shown in Figure 12. The figure shows that the current undergoes increase from 5.5 A to 11 A (rms) and take 0.1 msec to reach its steady-state value. The

load power increases from 1200 W to 2380 W. The output voltage (v_c) waveform is shown in Figure 13. The figure shows that there is a slight effect on the load voltage due to this sudden load change. The THD of the output voltages is 1.55% as shown in Figure 14. The DC-link capacitor voltage (v_{inv}) is shown in Figure 15. The figure shows that the DC-link voltage is slight affected by load change. The boosting inductor current (i_{dc}) is shown in Figure 16, which its average value has increased from 8.5 A to 17 A.

Table 1. Single-phase SSI system parameters

AC side	
Reference output voltage v_c^*	220 V rms
Frequency f	50 Hz
Switching Frequency f_c	10 KHz
Output filter inductor L_f	5 mH
Output filter capacitor C_f	100 μ F
Load resistance R_l	40 Ω
Load inductance L_l	10 mH
DC-Link side	
DC-source	140 V
DC-link voltage	500 V
DC-link capacitor C_{dc}	2000 μ F
DC-link input inductor L_{dc}	3 mH

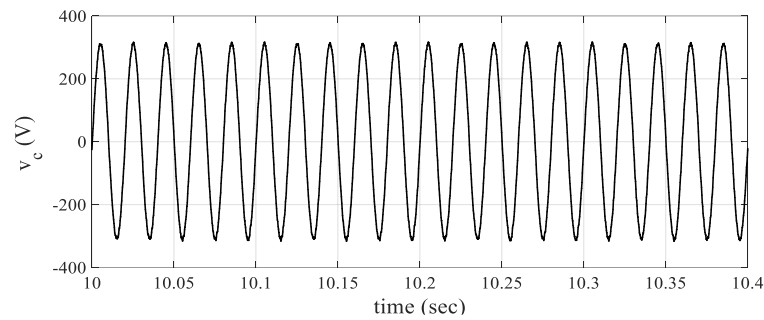


Figure 7. The AC load voltage (v_c)

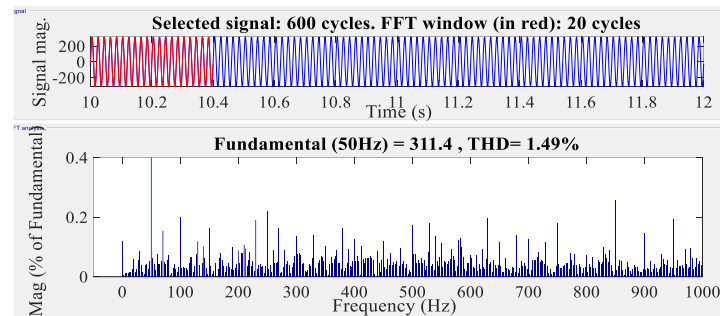


Figure 8. THD of the AC load voltage (v_c)

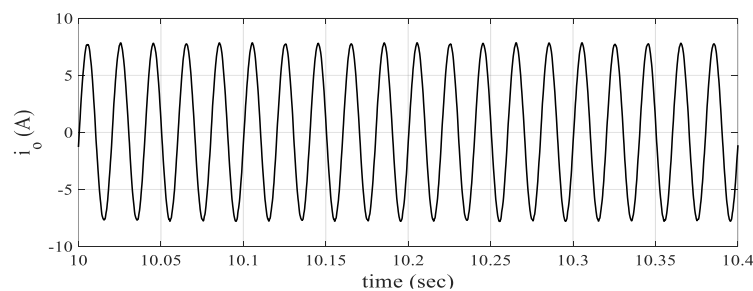
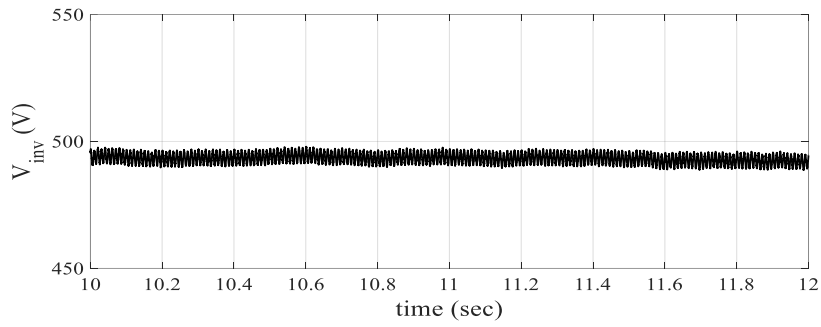
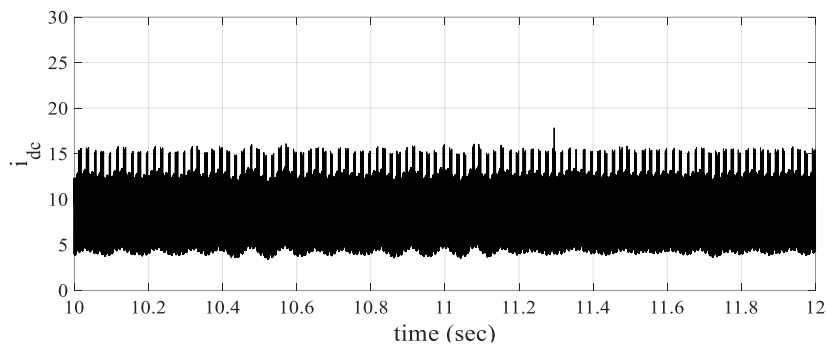
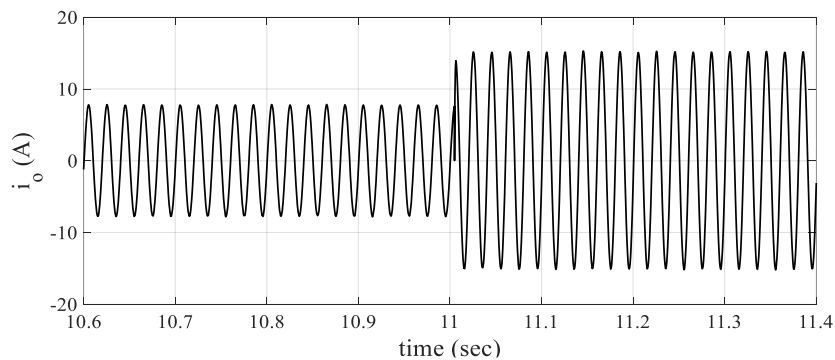
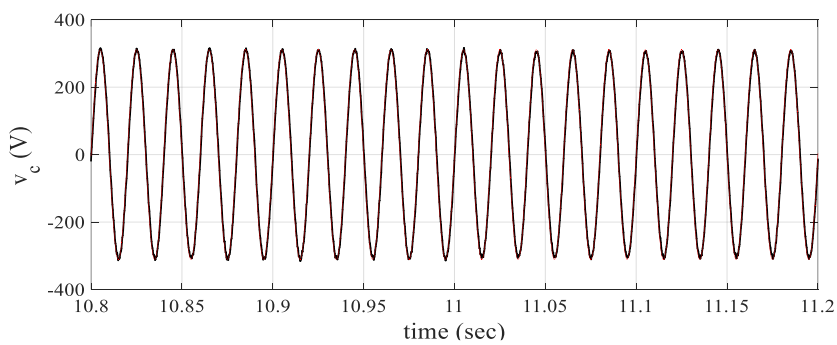


Figure 9. The AC load current (i_o)

Figure 10. The DC-link voltage (V_{inv})Figure 11. The DC input current (i_{dc})Figure 12. The AC load current (i_o) at 100% step load changeFigure 13. The AC load voltage (v_c) at 100% step load change

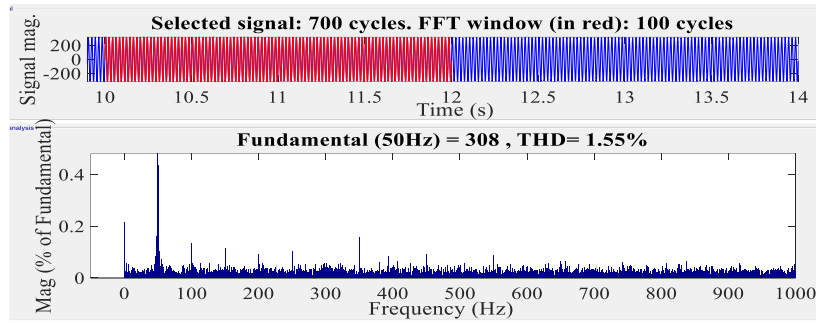


Figure 14. THD of the AC load voltage (v_c) at 100% step load change

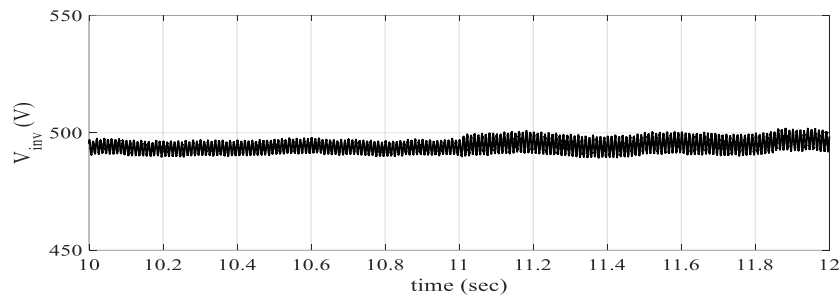


Figure 15. The DC-link voltage (V_{inv}) at 100% step load change

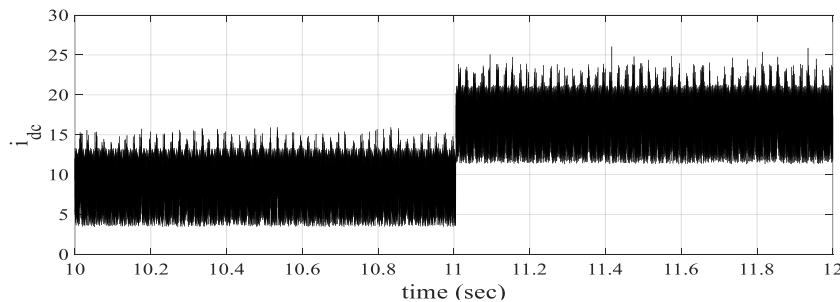


Figure 16. The DC input current (i_{dc}) at 100% step load change

5. CONCLUSION

In this paper single-phase split-source inverter (SSI) has been controlled by a modified FCS-MPC based on Harris Hawks optimization. The AC load voltage, the DC-link voltage, and the DC input current are controlled simultaneously. Weighting factors determine the importance of each term within the cost function and are obtained using Harris Hawks optimization technique. The SSI performance is validated under a certain load, which consume 1200 W. The results show that the AC load voltage is well regulated with low THD (1.49%), and the input power is controlled while maintaining the DC-link voltage content with low ripples (2%). The system is also simulated under 100% load change, which the load consumes 2380 W. The results show that FCS-MPC has a high-performance response. In both cases, the DC input current has high ripples (8.5 A ripples) as it has a low weighting factor. As the DC input current weighting factor increases, as the THD of the AC voltage and ripples of the DC-link voltage increases too. The FCS-MPC algorithm sacrifices the DC input current to regulate the AC and DC voltages.




REFERENCES

- [1] A. Stone, M. Rasheduzzaman, and P. Fajri, "A Review of Single-Phase Single-Stage DC/AC Boost Inverter Topologies and Their Controllers," *IEEE Conference on Technologies for Sustainability (SusTech)*, Long Beach, CA, USA, pp. 1-8, Nov. 2018, pp. 1-8, doi: 10.1109/SusTech.2018.8671380.




- [2] S. D. S. Nunna, A. Ketha, S. S. G. Padamat, K. Rambabu, U. A. Kshirsagar, A. Tirupathi, "A single-phase simplified DC-AC converter using DC-link capacitors and an H-bridge," *Bulletin of Electrical Engineering and Informatics*, vol. 10, no. 6, pp. 2964–2971, Dec. 2021, doi: 10.11591/eei.v10i6.2788.
- [3] O. Ellabban and H. Abu-Rub, "Z-source inverter: Topology improvements review," *IEEE Ind. Electron. Mag.*, vol. 10, no. 1, pp. 6–24, Mar. 2016, doi: 10.1109/MIE.2015.2475475.
- [4] Y. Siwakoti, F. Z. Peng, F. Blaabjerg, P. C. Loh, and G. Town, "Impedance source networks for electric power conversion part I: A topological review," *IEEE Trans. Power Electron.*, vol. 30, no. 2, pp. 699–716, Feb. 2015, doi: 10.1109/TPEL.2014.2313746.
- [5] V. Saravanan, M. Aravindan, V. Balaji, M. Arumugam, "Z Source Inverter Topologies-A Survey," *Bulletin of Electrical Engineering and Informatics*, vol. 6, no. 1, pp. 1–12, Mar. 2017, doi: 10.11591/eei.v6i1.579.
- [6] C. R. Balamurugan, K. Vijayalakshmi, "Comparative Analysis of Various Z-source Based Five Level Cascaded H-bridge Multilevel Inverter," *Bulletin of Electrical Engineering and Informatics*, vol. 7, no. 1, pp. 1–14, Mar. 2018, doi: 10.11591/eei.v7i1.656.
- [7] Y. P. Siwakoti, F. Z. Peng, F. Blaabjerg, P. C. Loh, G. E. Town, and S. Yang, "Impedance-source networks for electric power conversion part II: Review of control and modulation techniques," *IEEE Trans. Power Electron.*, vol. 30, no. 4, pp. 1887–1906, Apr. 2015, doi: 10.1109/TPEL.2014.2329859.
- [8] A. Nahavandi, M. Roostaei, and M. R. Azizi, "Single stage dc-ac boost converter," in *Proc. 7th Power Electron., Drive Syst. Technol. Conf.*, pp. 362–366, Tehran, Iran, 16–18 Feb. 2016, doi: 10.1109/PEDSTC.2016.7556888.
- [9] A. Abdelhakim, P. Mattavelli, P. Davari, and F. Blaabjerg, "Performance evaluation of the single-phase split-source inverter using an alternative dc-ac configuration," *IEEE Trans. Ind. Electron.*, vol. 65, no. 1, pp. 363–373, Jan. 2018, doi: 10.1109/TIE.2017.2714122.
- [10] S. S. Lee, A. S. T. Tan, D. Ishak, and R. Mohd-Mokhtar, "Single-Phase Simplified Split-Source Inverter (S³I) for Boost DC-AC Power Conversion," *IEEE Trans. Ind. Electron.*, vol. 66, no. 10, pp. 7643–7652, Oct. 2019, doi: 10.1109/TIE.2018.2886801.
- [11] S. S. Lee and Y. E. Heng, "Improved single-phase split-source inverter with hybrid quasi-sinusoidal and constant PWM," *IEEE Trans. Ind. Electron.*, vol. 64, no. 3, pp. 2024–2031, Mar. 2017, doi: 10.1109/TIE.2016.2624724.
- [12] C. Yin, W. Ding, L. Ming and P. C. Loh, "Single-Stage Active Split-Source Inverter with High DC-Link Voltage Utilization," *IEEE Trans. Power Electron.*, vol. 36, no. 6, pp. 6699–6711, June 2021, doi: 10.1109/TPEL.2020.3038688.
- [13] A. Bakeer, M. Ismail, M. Orabi, "A powerful finite control set-model predictive control algorithm for quasi-Z-source inverter," *IEEE Trans. Ind. Informat.*, vol. 12, no. 4, pp. 1371–1379, May 2016, doi: 10.1109/TII.2016.2569527.
- [14] S. Vazquez, J. Rodriguez, M. Rivera, L. G. Franquelo, and M. Norambuena, "Model predictive control for power converters and drives: Advances and trends," *IEEE Trans. on Ind. Electron.*, vol. 64, no. 2, pp. 935–947, Feb. 2017, doi: 10.1109/TIE.2016.2625238.
- [15] M. Nikroo, S. H. Montazeri, J. Milimonfared, and F. Shadian, "Performance Analysis of Model Predictive Controller for Grid-Connected Quasi Z-Source and Split-Source PV Inverters," *11th Power Electronics, Drive Systems, and Technologies Conference (PEDSTC)*, pp. 1–6, Tehran, Iran, 4–6 Feb. 2020, doi: 10.1109/PEDSTC49159.2020.9088463.
- [16] J. Rodriguez and P. Cortes, "Predictive control of power converters and electrical drives," *John Wiley & Sons, Ltd.*, Publication, ISBN: 978-1-119-96398-1, United Kingdom: Wiley-IEEE Press, 2012, pp. 1–227.
- [17] S. Vazquez, J. I. Leon, L. G. Franquelo, J. R. Iguéz, H. A. Young, A. Marquez, and P. Zanchetta, "Model Predictive Control A Review of Its Applications in Power Electronics," *IEEE Ind. Electron. magazine*, pp. 16–31, Mar. 2014, doi: 10.1109/MIE.2013.2290138.
- [18] A. Yousfi, Y. Bot, F. Mehedi, and A. Chaker, "Current model predictive control for three-phase active power filter using cascaded H-bridge multilevel converter," *Indonesian Journal of Electrical Engineering and Computer Science*, vol. 21, no. 2, pp. 714–722, Feb. 2021, doi: 10.11591/ijeecs.v21.i2.pp714-722.
- [19] R. G. Omar, "Modified FCS-MPC algorithm for five-leg voltage source inverter," *Indonesian Journal of Electrical Engineering and Computer Science*, vol. 19, no. 1, pp. 47–57, July 2020, doi: 10.11591/ijeecs.v19.i1.pp47-57.
- [20] Z. Massaq, A. Abounada, and M. Ramzi, "Fuzzy and predictive control of a photovoltaic pumping system based on three-level boost converter," *Bulletin of Electrical Engineering and Informatics*, vol. 10, no. 3, pp. 1183–1192, June 2021, doi: 10.11591/eei.v10i3.2605.
- [21] P. Cortés, G. Ortiz, J. I. Yuz, J. Rodríguez, S. Vazquez, and L. G. Franquelo, "Model Predictive Control of an Inverter with Output LC Filter for UPS Applications," *IEEE Trans. on Ind. Electron.*, vol. 56, no. 6, pp. 1875–1883, June 2009, doi: 10.1109/TIE.2009.2015750.
- [22] R. O. Ramirez, J. R. Espinoza, F. Villarroel, E. Maurelia, and M. E. Reyes, "A novel hybrid finite control set model predictive control scheme with reduced switching," *IEEE Trans. on Ind. Electron.*, vol. 61, no. 11, pp. 5912–5920, Nov. 2014, doi: 10.1109/IECON.2013.6700080.
- [23] P. Cortes, L. Vattuone, and J. Rodriguez, "Predictive Current control with reduction of switching frequency for three phase voltage source inverters," in *IEEE International Symposium on Industrial Electronics*, pp. 1817–1822, Gdansk, Poland, 27–30 June 2011, doi: 10.1109/ISIE.2011.5984433.
- [24] Y. Elthokaby, and N. Abdel-Rahim, "Two-Step Finite-Control Set Model Predictive Control for Three Phase UPS Inverters Feeding Non-linear Loads," *21st European Conference on Power Electronics and Applications (EPE '19 ECCE Europe)*, Genova, Italy, 3–5 Sept. 2019, doi: 10.23919/EPE.2019.8914862.
- [25] M. A. Ismail, "High Dynamic Performance for Split-Source Inverter based on Finite Control Set Model Predictive Control," *21st International Middle East Power Systems Conference (MEPCON)*, pp. 8–13, Tanta University, Egypt, 17–19 Dec. 2019, doi: 10.1109/MEPCON47431.2019.9007972.
- [26] G. M. Cocco, J. d. A. Borges, M. Stefanello and F. B. Grigoletto, "Finite Set Model Predictive Control of Four-Leg Split-Source Inverters," *13th IEEE International Conference on Industry Applications (INDUSCON)*, pp. 630–635, Sao Paulo, Brazil, 12–14 Nov. 2018, doi: 10.1109/INDUSCON.2018.8627303.
- [27] J. de Azevedo Borges and F. B. Grigoletto, "Finite set model predictive control of grid connected split-source inverters," *Brazilian Power Electronics Conference (COBEP)*, pp. 1–6, Juiz de Fora, Brazil, 19–22 Nov. 2017, doi: 10.1109/COBEP.2017.8257297.
- [28] A. A. Heidari, S. Mirjalili, H. Faris, I. Aljarah, M. Mafarja, and H. Chen, "Harris hawks optimization: Algorithm and applications," *Future Generation Computer Systems*, vol. 97, pp. 849–872, Aug. 2019, doi: 10.1016/j.future.2019.02.028.
- [29] X. Bao, H. Jia, and C. Lang, "A novel hybrid Harris hawks' optimization for color image multilevel thresholding segmentation," *IEEE Access*, vol. 7, pp. 76529–76546, June 2019, doi: 10.1109/ACCESS.2019.2921545.

BIOGRAPHIES OF AUTHORS






Youssuf Elthokaby    received the B.Sc. and M.Sc. degrees in electrical engineering from the Faculty of Engineering at Shoubra, Benha University, Egypt, in 2014 and 2017, respectively. He is an Assistant Lecturer in Shoubra Faculty of Engineering, where he assists in teaching several power electronics courses. Since 2019, he has been working toward the Ph.D. degree in power electronics under the supervision of Prof. Naser Abdel-Rahim. His research interests include analysis, modeling, control, and investigation of new power converter topologies for renewable energy systems. He can be contacted at email: youssef.hassan@feng.bu.edu.eg.






Ibrahim Abdelsalam    (Senior Member, IEEE) received the B.Sc. degree (Hons.) in electrical engineering from the Arab Academy for Science and Technology and Maritime Transport, Alexandria, Egypt, in 2006, the M.Sc. degree in electrical engineering from the Arab Academy for Science and Technology and Maritime Transport, Cairo, Egypt, in 2009, and the PhD degree in power electronics from the University of Strathclyde, Glasgow, U.K., 2016. He is currently an Associate Professor with the Department of Electrical Engineering, Arab Academy for Science and Technology and Maritime Transport. He can be contacted at email: I.abdelsalam@aast.edu.



Naser Abdel-Rahim Ph.D.   , currently holds the position of Professor in the Department of Electrical Engineering of Future University in Egypt. From 2013 to 2017, he had been a Professor with the Faculty of Engineering at Shoubra, Benha University, Egypt. He received both the M. Eng. and Ph.D. degrees from the Memorial University of Newfoundland in Canada, in 1989 and 1995, respectively. As an Assistant Professor at the United Arab Emirates University (UAEU) from 2000 till 2005, he obtained several research projects funding from the UAEU as well as from Asea Brown Boveri (ABB). Prof. Abdel-Rahim has numerous publications in international journals and refereed conferences, where he also served as reviewer. He can be contacted at email: naser.abdelrahim@fue.edu.eg.



Islam Mohamed Abdealqawee    is an Assistant Prof. at the Department of Electrical engineering, Faculty of Engineering at Shoubra, Benha University, Egypt. He received his B.Sc. (2008) degree from Department of Electrical engineering, Faculty of Engineering at Shoubra, Benha University and M.Sc. (2014) degree and Ph.D. (2019) degree from the same University. He has research papers about the renewable energy, optimization, and power electronics. He can be contacted at email: islam.ahmed@feng.bu.edu.eg.